Engineering Science and Technology, an International Journal 19 (2016) 1390–1399

HOSTED BY

Contents lists available at ScienceDirect

Engineering Science and Technology, an International Journal

journal homepage: www.elsevier.com/locate/jestch

A similarity solution for phase change of binary alloy with shrinkage or expansion

A. Jakhar, P. Rath, S.K. Mahapatra *

School of Mechanical Sciences, IIT Bhubaneswar, Bhubaneswar 751013, India

ARTICLE INFO

Article history:
Received 11 January 2016
Accepted 1 April 2016
Available online 23 April 2016

Keywords:
Binary alloy
Single phase
Density ratio
Lewis number
Solid–liquid interface

ABSTRACT

A similarity solution for solidification of an undercooled binary alloy is developed including the effect of shrinkage or expansion due to change in the density. The proposed similarity solution takes into account the change in density of the alloy while undergoing a phase change. Thermo-physical properties are assumed to be constant. An analytical solution (which is an outcome of the similarity solution) for temperature and concentration distribution has been established. The effect of the density ratio and Lewis number on both interface motion and conjugate heat and mass transfer is studied. It is found that the interface moves faster with the decrease in density ratio and initial temperature during solidification.

1. Introduction

The term phase is used as a synonym for state of matter which is uniform throughout both in chemical composition and physical state and is separated from another phase by a phase boundary. The phase change process involves solidification and melting and has myriad applications. The most common phase change processes are the formation of ice, the solidification of metals (especially in castings) and in cryogenics. In these processes, the solid–liquid interface is in motion, which involves simultaneous heat and mass transfer, both within the respective individual phases and at the solid–liquid interface. The first phase change process to be reported was studied by Stefan [18]. The time taken for solidification in lakes during winters was studied by Stefan with the help of simple mathematical tools. Thereafter, simple benchmark phase change problems started being referred as Stefan problems. The solution of the Stefan problem can be analytical or numerical. The analytical solution is restricted to the simplified one dimensional case. Özişik [16,15] and Yener [22] have carried out pioneer work in this area. The other one involves the numerical and the hybrid numerical solutions. The numerical solutions are of two types. The first one is the front tracking method and the second one is the fixed domain method, which is most commonly used in numerical applications. Some of the numerical method types are the specific heat method, the effective specific heat method, the enthalpy method, the source based methods, the temperature recovery method and the heat integration method.

In the binary alloy solidification process, there exists a two phase zone consisting of both liquid and solid phases called as the mushy zone. Numerous models have been developed for the solidification processes involving mushy zone, to study the effect of macro segregation, micro segregation and dendrite formation. The first analytical solution for binary alloys was proposed by Rubinstein [17] and later improved by Alexiades [2]. In these studies, a semi-infinite domain having a fixed boundary temperature with uniform composition and temperature was taken as an initial condition. Further, extended work has been carried by Tien and Geiger [19], Crowley and Ockendon [12], Bermudez and Saguez [5] and Chakraborty and Dutta [7,8]. In late 1980s, Incropera and Bennon [3,4] developed a continuum mixture model for the binary alloy solidification. They took two a dimensional rectangular cavity, subjected to insulated and fixed boundary conditions and studied macro-segregation phenomenon during solidification in binary alloy through their model. Subsequently, Christenson et al. [10,11] validated the numerical work of Incropera and Bennon [3,4] with their own experiments on NH_4Cl–H_2O binary mixture. Successively, Dutta and Chakraborty [7–9] have carried out extensive work on binary alloy phase change in which they have studied the effect of partition coefficient and several other parameters during phase change on macro-segregation patterns obtained for an alloy mixture using enthalpy method. With ease of implementation, the enthalpy method has got more popularity as compared to other methods and could be used quite extensively in the modeling the experimental work.

* Corresponding author.
E-mail address: swarup@iitbbs.ac.in (S.K. Mahapatra).
Peer review under responsibility of Karabuk University.

http://dx.doi.org/10.1016/j.jestch.2016.04.002

Nomenclature

C	solute concentration (%)
c	specific heat (J/kg K)
D	sass diffusivity (m^2/s)
k	thermal conductivity (W/m K)
k_p	partition coefficient
L_f	latent heat of fusion (J/kg)
L	length scale (m)
Le	Lewis number $(\frac{\alpha}{D})$
M	dimensionless Liquidus slope
R	ratio of densities of solid to liquid phase $(\frac{\rho_s}{\rho_l})$
s	position of the interface (m)
T	temperature in (K)

Greek symbols

α	thermal diffusivity (m^2/s)
ρ	density (kg/m^3)
λ	similarity parameter

Superscripts

$(^*)$	non-dimensional form of the equation

Subscripts

b	boundary
f	fusion point
i	interface
l	liquid phase
s	solid phase

Voller [20] developed an analytical solution for a single phase binary alloy of an undercooled liquid during solidification. Subsequently, using this analytical model, Voller [21] has validated the numerical model for dendritic growth in an undercooled static melt. But in practical cases, melt is convective during dendritic growth, which has been addressed by Bhattacharya and Dutta [6] in case of binary alloy. However, in modeling most practical cases, such as the phase change material as done by Agarwal and Sarviya [1] and in castings by Jafar-Salehi et al. [13], the effect of density change has not been taken into account, which is an unreasonable assumption. There is significant density change of approximately 2–20% for most metal and alloys and −5% to −15% for water and polymers during solidification [14]. If we take the above mentioned effect in the problem, it is expected that the density change will significantly affect the solid–liquid interface motion. The present paper is an extension of the work carried out by Voller [20], assuming the interface to be sharp. In the case of the work carried out by Voller [20], density is taken constant and invariant with phase change, while in current problem density is assumed to be constant but it is different for solid and liquid phases. In the current problem, the effect of density ratio and Lewis number has been studied on the solid–liquid interface motion along with temperature and concentration distribution. In addition, the effect of initial and boundary temperature on binary alloy phase change behavior is also studied in this proposed model.

2. Problem description

The problem formulation consists of a one dimensional Stefan problem in a semi-infinite domain as shown in Fig. 1 in which the density of solid and liquid are assumed to be different, although it is constant in the respective pure phases. Initially, the liquid melt (Fig. 1(a)) is kept at a uniform undercooled temperature $T_l = T_o$ and at uniform concentration $C_l = C_o$. The solidification is initiated by keeping a small metal strip at the melting point on the left boundary (Fig. 1(b)), which provides a temperature gradient and serves as driving force for solidification. During solidification, the heat and mass transfer takes place across phase interface. The latent and sensible heat starts flowing from the liquid phase to the solid phase and the solute concentration goes on increasing in the liquid phase due to the partition of solute in the solid and the liquid phase at the interface and mass diffusion within them.

Following assumptions are taken while preparing the model for solidification system.

1. The thermo-physical properties like thermal conductivity, specific heat and mass diffusivity are assumed to be invariant with temperature and concentration change for liquid and solid phases.
2. The concentration and temperature variation is only along the direction of solidification.
3. Heat and mass diffusion in solid is neglected.
4. The phase change heat transfer is assumed conduction dominated and effects due to buoyancy are neglected.
5. The interface is assumed to be sharp and straight for the entire period of solidification.
6. The temperature and concentration relation at the interface is given by the liquidus slope of the binary phase diagram.
7. Surface tension and capillary effects are assumed to be absent.

Based on the above assumptions, the transport equations governing the solidification of a binary alloy can be represented as given below.

$$\frac{\partial T_l}{\partial t} + \left(\frac{\rho_s}{\rho_l} - 1\right)\frac{ds}{dt}\frac{\partial T_l}{\partial x} = \alpha_l \frac{\partial^2 T_l}{\partial x^2}, \quad x > s(t) \quad \text{(Liquid phase energy equation)} \tag{1}$$

$$\frac{\partial C_l}{\partial t} + \left(\frac{\rho_s}{\rho_l} - 1\right)\frac{ds}{dt}\frac{\partial C_l}{\partial x} = D_l \frac{\partial^2 C_l}{\partial x^2}, \quad x > s(t) \quad \text{(Liquid phase species transport equation)} \tag{2}$$

From mass and energy balance at the interface from the conservation principle, the interface condition governing the displacement of the interface can be expressed as:

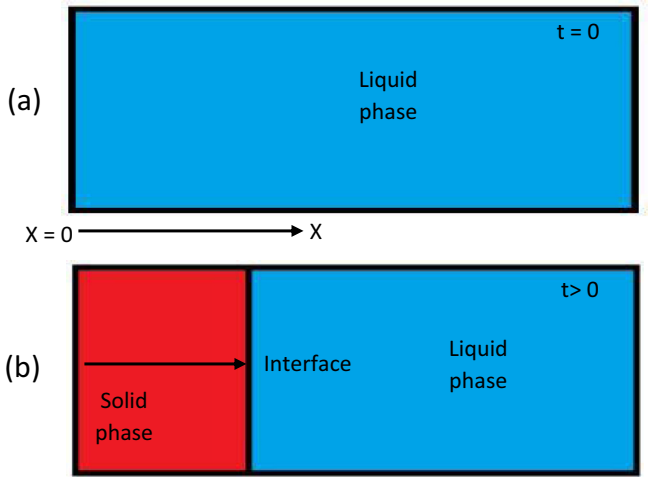

Fig. 1. The problem domain with respective phases at (a) initial time (b) at a given time during solidification.

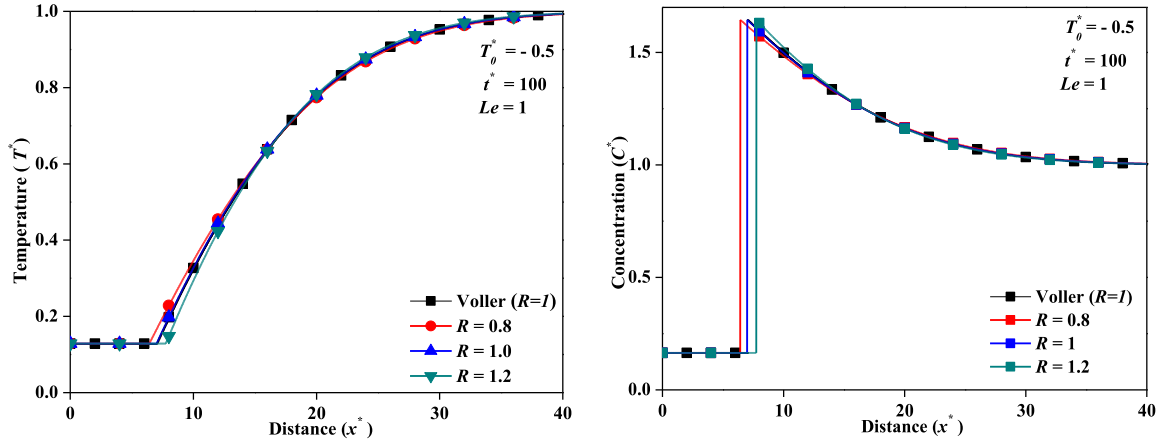

Fig. 2. Effect of density ratio on temperature and concentration distribution at $t^* = 100$.

$$-K_l\frac{\partial T_l}{\partial x} = \rho_s L\frac{\partial s}{\partial t},\ x = s(t) \quad \text{(Energy interface condition)} \tag{3}$$

$$-\rho_l D_l\frac{\partial C_l}{\partial x} = \rho_s C_{l,i}(1-k_p)\frac{\partial s}{\partial t},\ x = s(t) \quad \text{(Mass interface condition)} \tag{4}$$

The above Eqs. (1)–(4) expressed in non-dimensional forms using the following dimensionless parameters:

$$T^* = \frac{T - T_f - mC_o}{L_f/C_p},\ C^* = \frac{C}{C_o},\ x^* = \frac{x}{L},\ s^* = \frac{s}{L},\ t^* = \frac{\alpha_l t}{L^2} \tag{5}$$

Substituting the above dimensionless variables in the governing equations (Eqs. (1) and (2)), the non-dimensional form of the transport equations can be expressed as:

$$\frac{\partial T_l^*}{\partial t^*} + \left(\frac{\rho_s}{\rho_l} - 1\right)\frac{ds^*}{dt^*}\frac{\partial T_l^*}{\partial x^*} = \frac{\partial^2 T_l^*}{\partial x^{*2}},$$
$$x^* > s^*(t^*) \quad \text{(Liquid phase energy equation)} \tag{6}$$

$$\frac{\partial C_l^*}{\partial t^*} + \left(\frac{\rho_s}{\rho_l} - 1\right)\frac{ds^*}{dt^*}\frac{\partial C_l^*}{\partial x^*} = \frac{1}{Le}\frac{\partial^2 C_l^*}{\partial x^{*2}},$$
$$x^* > s^*(t^*) \quad \text{(Liquid phase species transport equation)} \tag{7}$$

The temperature of the liquid and the solid phase at the interface $x^* = s^*(t^*)$ is given as $T_l^* = T_s^* = T_i^*$ and the concentration of the solute in liquid and solid phase at the interface is maintaining a fixed ratio based on the partition coefficient as $C_{s,i}^* = k_p C_{l,i}^*$. The temperature and concentration at the interface are related as $T_i^* = MC_o(1 - C_{l,i}^*)$. The interface condition in the dimensionless form is given as:

$$-\frac{\rho_l}{\rho_s}\frac{\partial T_l^*}{\partial x^*} = \frac{\partial s^*}{\partial t^*},\ x^* = s^*(t^*) \quad \text{(Energy interface condition)} \tag{8}$$

$$-\frac{1}{Le}\frac{\rho_l}{\rho_s}\frac{\partial C_l^*}{\partial x^*} = C_{l,i}^*(1-k_p)\frac{\partial s^*}{\partial t^*},$$
$$x^* = s^*(t^*) \quad \text{(Mass interface condition)} \tag{9}$$

3. Similarity solution

The similarity solution for position of the interface would be given by $s^* = 2\lambda\sqrt{t^*}$, where λ is the similarity parameter. Solving Eqs. (6) and (7) analytically using this similarity parameter results in following temperature and concentration distribution in the domain:

$$T_s^* = T_i^*,\ 0 < x^* < s^*(t^*) \quad \text{(Solid phase)} \tag{10}$$

$$T_l^* = T_0^* + (T_i^* - T_0^*)\frac{\operatorname{erfc}\left(\frac{x^*}{2\sqrt{t^*}} - \lambda(R-1)\right)}{\operatorname{erfc}(\lambda(2-R))},$$
$$x^* > s^*(t^*) \quad \text{(Liquid phase)} \tag{11}$$

$$C_s^* = k_p C_{l,i}^*,\ 0 < x^* < s^*(t^*) \quad \text{(Solid phase)} \tag{12}$$

$$C_l^* = C_0^* + (C_{l,i}^* - C_0^*)\frac{\operatorname{erfc}\left(\frac{x^*\sqrt{Le}}{2\sqrt{t^*}} - \lambda(R-1)\right)}{\operatorname{erfc}(\lambda\sqrt{Le} - \lambda(R-1))},$$
$$x^* > s^*(t^*) \quad \text{(Liquid phase)} \tag{13}$$

Putting T_i^* and $C_{l,i}^*$ obtained from the above equations in the expression $T_i^* = MC_o(1 - C_{l,i}^*)$ results in a non-linear equation of λ which is solved using Newton Raphson method. The derivation has been given in the appendix.

4. Validation

The present similarity solution has been compared with the one phase, a single component analytical solution with no density change, as done by Özişik [15]. In the present problem, this can be achieved by setting the partition coefficient $k_p = 1$, concentration to be uniform initially which leads to $C_o^* = 1$ and the density change to be absent ($R = 1$). Using these conditions, the problem becomes a simple one dimensional, one phase, one component Stefan problem whose solution can be readily obtained as described below. The governing equation and interface condition for this benchmark Stefan problem is given by the expressions mentioned in the equations given below,

$$\frac{\partial T_l^*}{\partial t^*} = \frac{\partial^2 T_l^*}{\partial x^{*2}},\ s^*(t^*) < x^* < \infty \quad \text{(Liquid phase)} \tag{14}$$

$$-\frac{\partial T_l^*}{\partial x^*} = \frac{\partial s^*}{\partial t^*},\ x^* = s^*(t^*),\ s^*(t) = 2\lambda\sqrt{t^*} \tag{15}$$

$$\text{velocity of interface} = \frac{ds^*}{dt^*} = \frac{\lambda}{\sqrt{t^*}} \tag{16}$$

After taking into consideration, the heat transport and interface equation from Eqs. (14) and (15), we get the analytical expressions for the temperature distribution in the liquid phase given by Eq. (17).

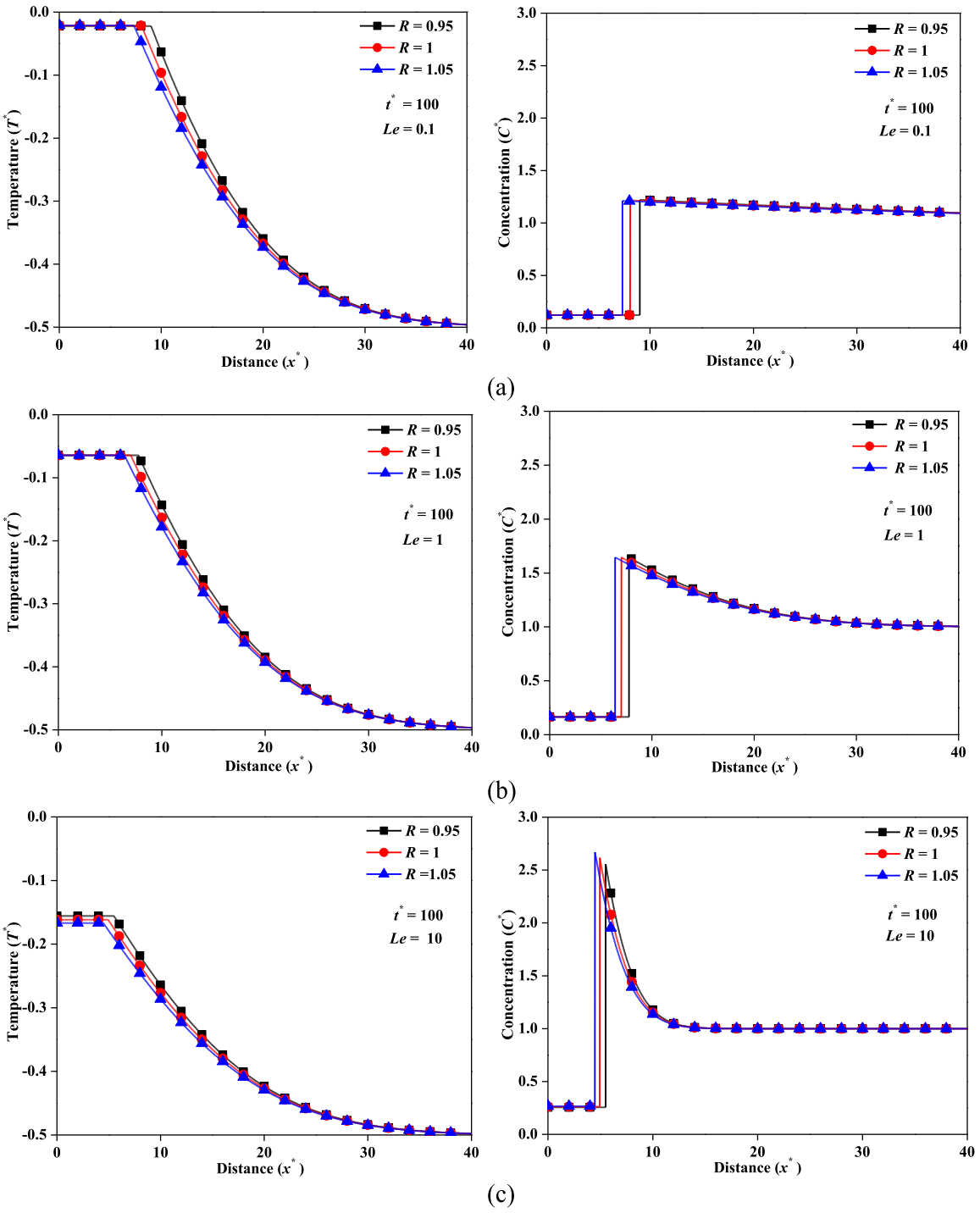

Fig. 3. Effect of density ratio (R) on temperature and concentration distribution at t^* = 100 for three different thermal-mass diffusion ratio (Le): (a) Le = 0.1; (b) Le = 1.0 and (c) Le = 10.

$$T_l^* = T_o^* + (T_i^* - T_o^*)\frac{\operatorname{erfc}\left(\frac{x^*}{2\sqrt{t^*}}\right)}{\operatorname{erfc}(\lambda)},\ x^* > s^*(t^*) \quad \text{(Liquid phase)} \qquad (17)$$

Eq. (17) can also be obtained by substituting $R = 1$ in Eq. (11). Substituting the above expressions in Eq. (15) and taking the melting point to be invariant, results in the equation for λ given as:

$$\lambda\sqrt{\pi}e^{\lambda^2}\operatorname{erfc}(\lambda) + T_o^* = 0 \qquad (18)$$

Eq. (18) can also be obtained from Eq. (A.10) for $R = 1$ which validates the proposed formulation. The proposed model is further validated with Voller [20] for solidification of an undercooled binary alloy using the similar boundary and initial conditions with no change in density during phase change as shown in Fig. 2.

5. Results and discussion

The results are discussed here to study the effect of Le, R, T_o^* and λ on solidification of the undercooled melt. The value of both k_p and M is kept as to 0.1.

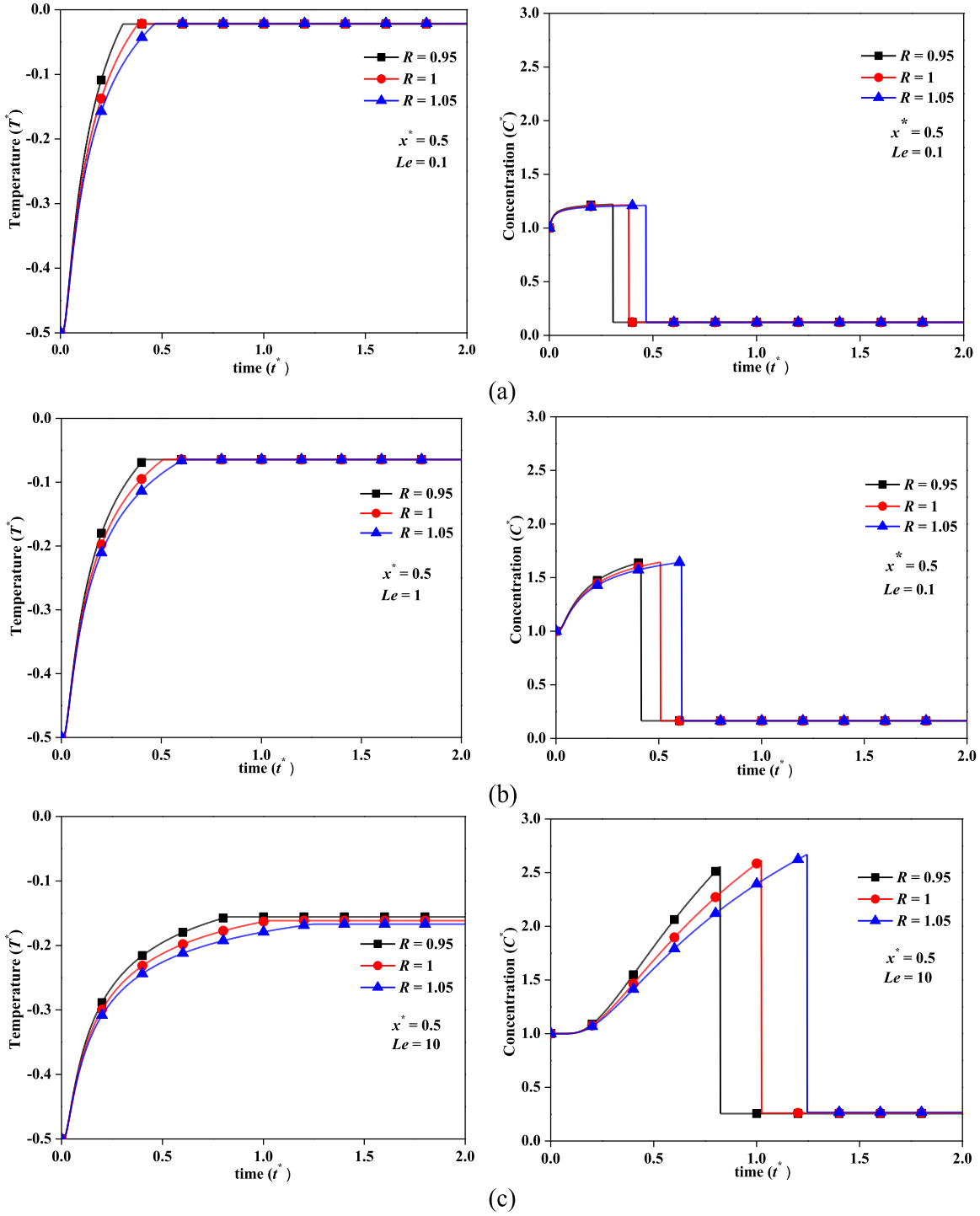

Fig. 4. Effect of density ratio (R) on transient variation of temperature and concentration at a given location (x^* = 0.5) for three different thermal-mass diffusion ratio (Le): (a) Le = 0.1; (b) Le = 1.0 and (c) Le = 10.

5.1. Effect of density ratio

Density ratio (R) is the most important factor affecting solidification, whose effect has been mainly studied in this article. Fig. 3 shows the effect of R on temperature and concentration distribution at t^* = 100 for different values of Le. Fig. 4 shows the effect of R on transient temperature and concentration distribution at a given location (x^* = 0.5). In Figs. 3 and 4, there is a sudden jump in the values of concentration of solute at the interface due to the partition of solute in solid and liquid phases respectively. This ratio of solute in solid to liquid at the interface is assumed to be fixed and called as the partition coefficient, k_p. Table 1(a) shows the position of interface at time, t^* = 100 while Table 1(b) tells us about the time taken for the solidification front to reach to a given location (x^* = 0.5) for different Lewis numbers and density ratio. On analyzing Table 1, it can be inferred that with a decrease in density ratio, the interface moves faster. This could be attributed to the fact that the decrease in the density ratio will increase the volume of liquid during solidification. It causes expansion in the solid domain and in order to accommodate it, the interface moves faster.

Table 1
Effect of density ratio (R) and Lewis number (Le) on: (a) solidification front position at a given time ($t^* = 100$), (b) time for the solidification front to reach to a given location ($x^* = 0.5$).

	Lewis number (Le)	Density ratio (R)		
		0.95	1.0	1.05
(a)				
Distance (x^*)	0.1	9.03	8.09	7.34
($t^* = 100$)	1.0	7.77	7.02	6.41
	10.0	5.52	4.96	4.50
(b)				
Time (t^*)	0.1	0.31	0.38	0.47
($x^* = 0.5$)	1.0	0.42	0.51	0.61
	10.0	0.82	1.02	1.25

Table 2
Effect of Initial temperature (T_o^*) and Lewis number (Le) on solidification front position at a given time ($t^* = 100$).

	Lewis number (Le)	Initial temperature (T_o^*)		
		−0.8	−0.5	−0.2
Distance (x^*)	0.1	9.03	8.09	7.34
($t^* = 100$)	1.0	7.77	7.02	6.41
	10.0	5.52	4.96	4.50

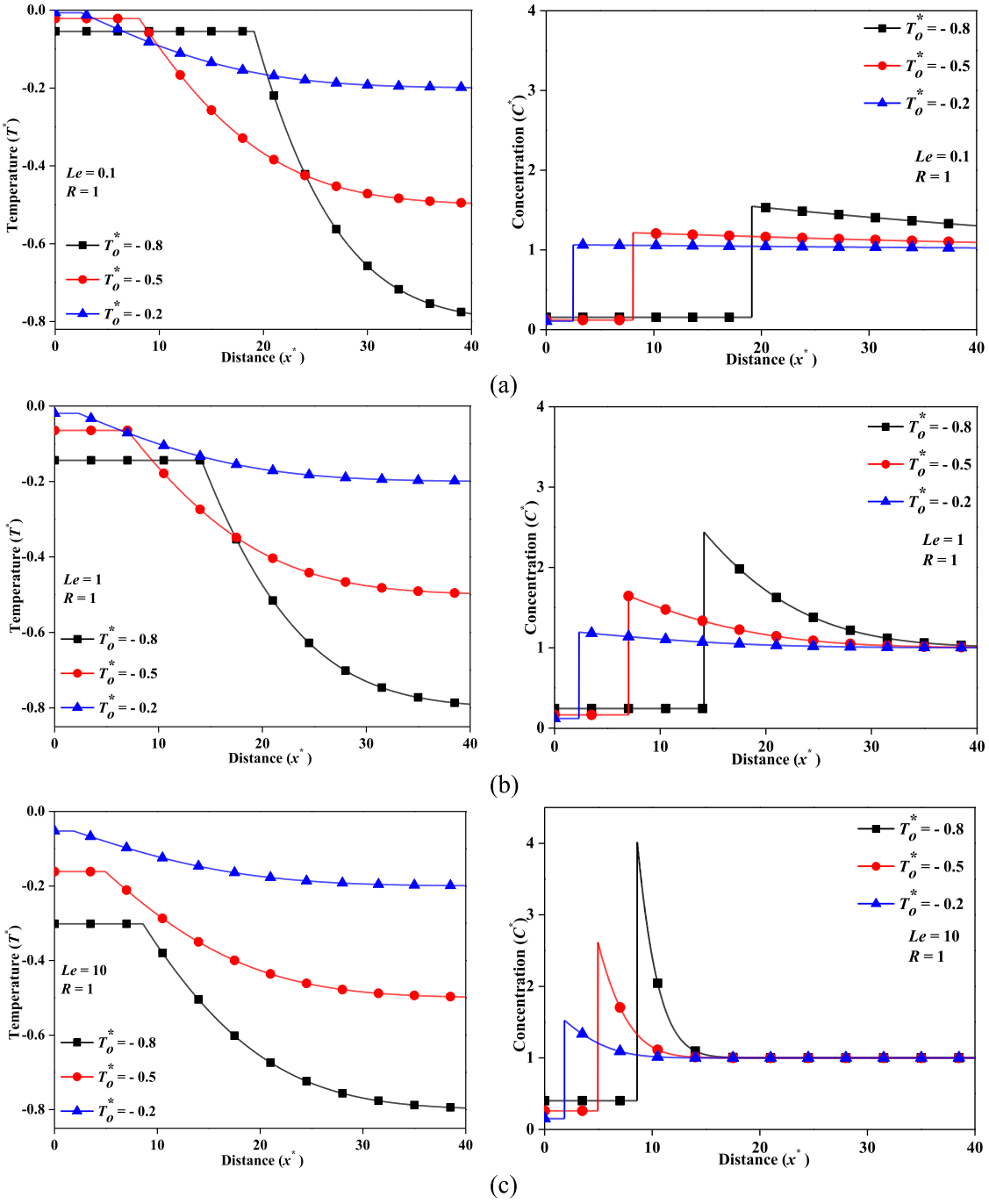

Fig. 5. Effect of initial temperature (T_o^*) on temperature and concentration distribution in the domain at $t^* = 100$ for three different thermal-mass diffusion ratio (Le): (a) $Le = 0.1$; (b) $Le = 1.0$ and (c) $Le = 10$.

Table 3
Effect of Initial temperature (T_o^*) and Density Ratio (R) on solidification front position at a given time (t^* = 100).

	Initial temperature (T_o^*)	Density ratio (R)		
		0.9	1.0	1.1
Distance (x^*) (t^* = 100)	−0.8	21.52	14.17	10.82
	−0.5	8.73	7.02	5.90
	−0.2	2.67	2.33	2.06

5.2. Effect of initial temperature

Initial temperature plays a crucial role on solidification behavior. The concentration and temperature distribution are shown in Fig. 5 at time t^* = 100 for different Lewis numbers and undercooled initial temperatures while keeping density ratio to be fixed at $R = 1$. In Tables 2 and 3 the effect of initial temperature on solidification front positions is studied at a given time (t^* = 100) for different Lewis numbers and density ratio. From Tables 2 and 3, it can be inferred that the interface moves faster with the decrease in the

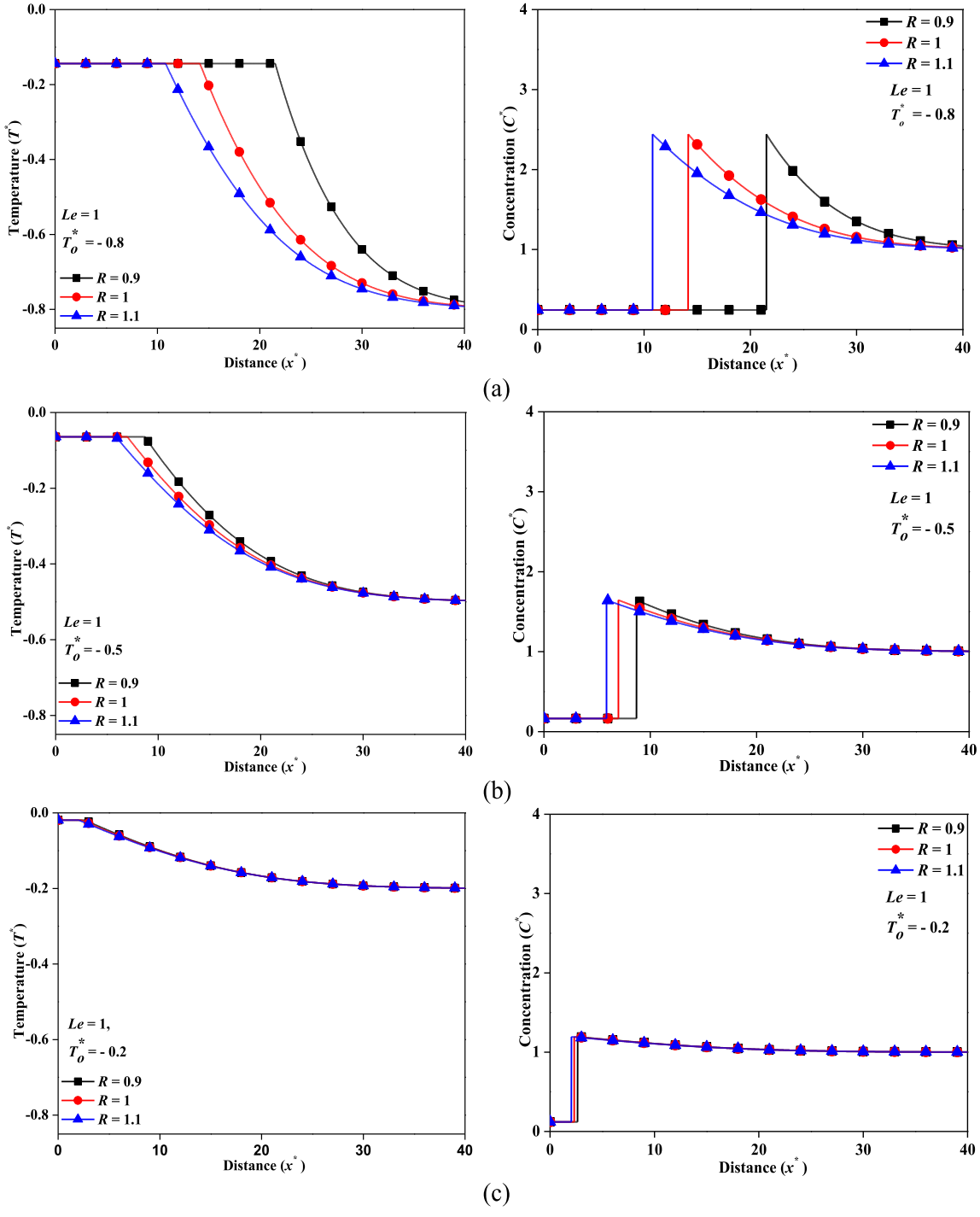

Fig. 6. Effect of density ratio (R) on temperature and concentration distribution in the domain at t^* = 100 for three different initial temperatures (T_o^*): (a) $T_o^* = -0.8$; (b) $T_o^* = -0.5$ and (c) $T_o^* = -0.2$.

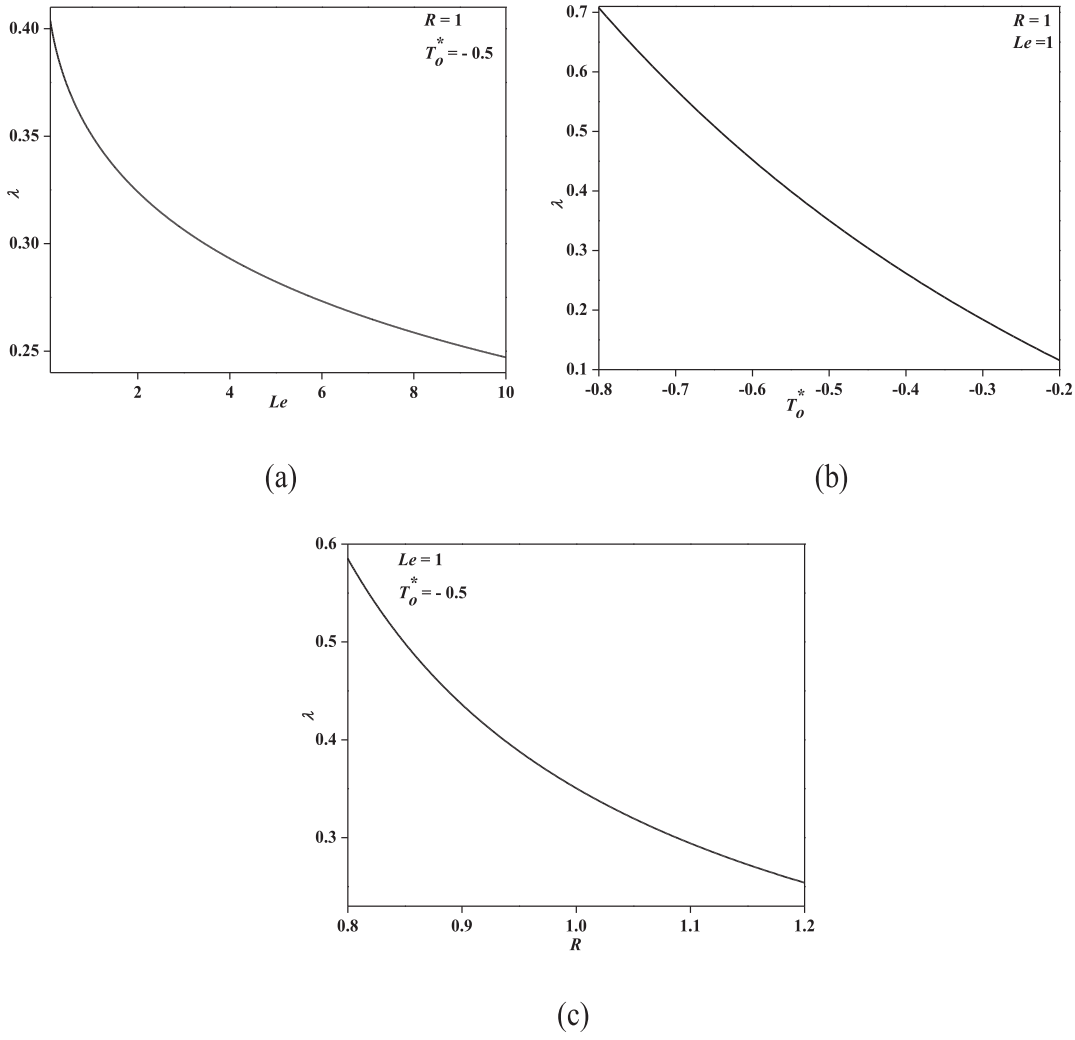

Fig. 7. Variation of similarity parameter (λ) with Le, T_o^* and R for three different cases: (a) $R = 1$, $T_o^* = -0.5$; (b) $Le = 1$, $R = 1$ and (c) $Le = 1$, $T_o^* = -0.5$.

value of undercooled initial temperature. As the initial temperature decreases, there is the rapid removal of heat for solidification to proceed, making the interface move faster. It can also be observed from Fig. 5 that the interface motion is highly sensitive to change in undercooled initial temperatures at the lower value of Lewis number. As Le decreases, the interface moves faster as endorsed from Eq. (9). With the decrease in Le, the rate of mass diffusion increases, which results in uniform distribution of solute concentration within the liquid phase. Fig. 6 shows the temperature and concentration distribution for different density ratio's and undercooled initial temperatures while keeping Lewis number to be fixed at $Le = 1$. As expected, the interface moves faster as the undercooled initial temperature decreases.

5.3. Effect of similarity parameter on interface motion

Similarity parameter is proportional to the interface speed, which can be concluded from Eq. (16). Fig. 7 shows the variation of λ with Le, T_o and R. The parameter decreases with increase in Le as shown in Fig. 7(a), which says that interface moves slower with an increase in Lewis number. This is due to decrease in solutal diffusivity, making solutal diffusion more difficult and hence slowing down the interface motion. Fig. 7(b) shows that interface moves slower with an increase in undercooled initial temperature. As the undercooled temperature decreases, more heat will be liberated owing to rapid solidification and hence the interface moves faster. From Fig. 7(c) we can conclude that interface moves slower with an increase in density ratio. As the density ratio increases, there is a contraction in part of the volume containing solid, which pulls the liquid backwards, causing the interface to move slower.

5.4. Effect of Lewis number

The temperature and concentration distribution is affected significantly by the change in Lewis number. While comparing Figs. 3 (a)–(c) and 4(a)–(c) for different Lewis numbers (0.1, 1 and 10), the concentration distribution becomes more uniform with the decrease in Lewis number. The mass diffusivity increases compared to thermal diffusivity for a low value of Le. High mass diffusivity results in rapid diffusion of solute in liquid. Hence, the solute concentration distribution will be more uniform in the liquid region. Secondly, from Figs. 3, 4 and 7(a) we can see that the interface moves faster with a decrease in Lewis number. Change in Lewis number would directly affect the phase change temperature. From the liquidus line in the phase diagram, it can be inferred that as the Lewis number decreases, mass diffusion increases and hence concentration of solute decreases in the liquid phase near the interface which in turn increases the phase change temperature (T_i^*). Hence, solidification would take place more easily.

6. Conclusion

A similarity solution is developed to study the effect of density ratio on the solidification of undercooled melt in the binary alloy. Based on the results, it can be concluded that both *Le* and *R* plays a very important role on solidification rate and behavior. The interface moves faster with a decrease in the value of *R* during solidification. The concentration distribution becomes more non-uniform while temperature distribution becomes uniform and interface motion becomes slower with an increase in *Le*. Lastly, the degree of undercooling also affects the interface motion. The interface moves faster with an increase in the degree of undercooling.

Appendix A

A.1. Energy equation

$$\frac{\partial T_l^*}{\partial t^*}+\left(\frac{\rho_s}{\rho_l}-1\right)\frac{ds^*}{dt^*}\frac{\partial T_l^*}{\partial x^*}=\frac{\partial^2 T_l^*}{\partial x^{*2}},\ x^*>s^*(t^*)\quad\text{(Liquid phase)}\tag{A.1}$$

A.2. Mass transfer equation

$$\frac{\partial C_l^*}{\partial t^*}+\left(\frac{\rho_s}{\rho_l}-1\right)\frac{ds^*}{dt^*}\frac{\partial C_l^*}{\partial x^*}=\frac{1}{Le}\frac{\partial^2 C_l^*}{\partial x^{*2}},\ x^*>s^*(t^*)\quad\text{(Liquid phase)}\tag{A.2}$$

A.3. The interface condition

$$-\frac{\rho_l}{\rho_s}\frac{\partial T_l^*}{\partial x^*}=\frac{\partial s^*}{\partial t^*},\ x^*=s^*(t^*)\quad\text{(Energy interface equation)}\tag{A.3}$$

$$-\frac{1}{Le}\frac{\rho_l}{\rho_s}\frac{\partial C_l^*}{\partial x^*}=C_{l,i}^*(1-k_p)\frac{\partial s^*}{\partial t^*},\quad x^*=s^*(t^*)\quad\text{(Mass transport interface equation)}\tag{A.4}$$

The general solution for energy Eq. (A.1) would be given by:

$$T_l^*=A+B\ \text{erfc}\left(\frac{x^*}{2\sqrt{t^*}}-\lambda\left(\frac{\rho_s}{\rho_l}-1\right)\right),\ x^*>s^*(t^*)\quad\text{(Liquid phase)}\tag{A.5}$$

$$\text{As } x^*\to\infty,\ \text{erfc}\left(\frac{x^*}{2\sqrt{t^*}}-\lambda\left(\frac{\rho_s}{\rho_l}-1\right)\right)\to 0$$

So we would have $A=T_0^*$ *as* $x^*\to\infty$

$$\text{As } x^*\to s^*(t^*),\ \text{erfc}\left(\frac{x^*}{2\sqrt{t^*}}-\lambda\left(\frac{\rho_s}{\rho_l}-1\right)\right)\to\text{erfc}\left(\frac{s^*}{2\sqrt{t^*}}-\lambda\left(\frac{\rho_s}{\rho_l}-1\right)\right)=\text{erfc}\left(\lambda\left(2-\frac{\rho_s}{\rho_l}\right)\right)$$

So we would have $B=\frac{(T_i^*-T_0^*)}{\text{erfc}\left(\lambda\left(2-\frac{\rho_s}{\rho_l}\right)\right)}$ as $x^*\to s^*(t^*)$

$$T_l^*=T_0^*+(T_i^*-T_0^*)\frac{\text{erfc}\left(\frac{x^*}{2\sqrt{t^*}}-\lambda\left(\frac{\rho_s}{\rho_l}-1\right)\right)}{\text{erfc}\left(\lambda\left(2-\frac{\rho_s}{\rho_l}\right)\right)},\quad x^*>s^*(t^*)\quad\text{(Liquid phase)}\tag{A.6}$$

The general solution for mass transfer Eq. (A.2) would be given by:

$$C_l^*=A+B\ \text{erfc}\left(\frac{x^*\sqrt{Le}}{2\sqrt{t^*}}-\lambda\left(\frac{\rho_s}{\rho_l}-1\right)\right),\ x^*>s^*(t^*)\quad\text{(Liquid phase)}\tag{A.7}$$

$$\text{As } x^*\to\infty,\ \text{erfc}\left(\frac{x^*\sqrt{Le}}{2\sqrt{t^*}}-\lambda\left(\frac{\rho_s}{\rho_l}-1\right)\right)\to 0$$

So we would have $A=C_o^*$ as $x^*\to\infty$

$$\text{As } x^*\to s^*(t^*),\ \text{erfc}\left(\frac{x^*\sqrt{Le}}{2\sqrt{t^*}}-\lambda\left(\frac{\rho_s}{\rho_l}-1\right)\right)\to\text{erfc}\left(\frac{s^*\sqrt{Le}}{2\sqrt{t^*}}-\lambda\left(\frac{\rho_s}{\rho_l}-1\right)\right)=\text{erfc}\left(\lambda\sqrt{Le}-\lambda\left(\frac{\rho_s}{\rho_l}-1\right)\right)$$

So we would have $B=\frac{(C_{l,i}^*-C_0^*)}{\left(\text{erfc}\left(\lambda\sqrt{Le}-\lambda\left(\frac{\rho_s}{\rho_l}-1\right)\right)\right)}$ as $x^*\to s^*(t^*)$

$$C_l^*=C_0^*+(C_{l,i}^*-C_0^*)\text{erfc}\frac{\text{erfc}\left(\frac{x^*\sqrt{Le}}{2\sqrt{t^*}}-\lambda\left(\frac{\rho_s}{\rho_l}-1\right)\right)}{\left(\text{erfc}\left(\lambda\sqrt{Le}-\lambda\left(\frac{\rho_s}{\rho_l}-1\right)\right)\right)},\quad x^*>s^*(t^*)\quad\text{(Liquid phase)}\tag{A.8}$$

Similarity solution would be given by $s^*=2\lambda\sqrt{t^*}$ (A.9)

So solving Eqs. (A.3), (A.6) and (A.9) we would get the expression for T_i^* in terms of λ as variable and other constants.

A.4. Interface temperature

$$T_i^*=T_o^*+\sqrt{\pi}*R*\lambda*e^{((\lambda-\lambda*(R-1))^2)}*(\text{erf}(\lambda*(R-2))+1)\tag{A.10}$$

Similarly solving Eqs. (A.4), (A.8) and (A.9) we would get the expression for $C_{l,i}^*$ in terms of λ as variable and other constants.

A.5. Interface concentration

$$N1=(C_o^*(e^{-(\lambda\sqrt{Le}-\lambda*(R-1))^2}))$$

$$D1=(\sqrt{\pi}*\sqrt{Le}*R*(\text{erf}(\lambda*(\sqrt{Le})+\lambda*(R-1))-1))$$

$$D2=\left(\lambda*(k-1)-\frac{e^{-(\lambda\sqrt{Le}-\lambda*(R-1))^2}}{(\sqrt{\pi}*\sqrt{Le}*R*(\text{erf}(\lambda*(\sqrt{Le})+\lambda*(R-1))-1))}\right)$$

$$C_{l,i}^*=-\frac{N1}{D1*D2}\tag{A.11}$$

Using the phase diagram relation we would a relation given by:

$$T_i^*=MC_o^*(1-C_{l,i}^*)\tag{A.12}$$

Using Eqs. (A.10)–(A.12) we will get an equation that is a function of λ, which is the only variable. Thus we solve it using Newton Raphson's method. The value of λ is obtained would be substituted in Eqs. (A.6), (A.8) and (A.9) to obtain temperature, concentration and interface motion.

Appendix B

B.1. Derivation for η

$$\frac{\partial T_l^*}{\partial t^*}+\left(\frac{\rho_s}{\rho_l}-1\right)\frac{ds^*}{dt^*}\frac{\partial T_l^*}{\partial x^*}=\frac{\partial^2 T_l^*}{\partial x^{*2}},\ x^*>s^*(t^*)\quad\text{(Liquid phase)}\tag{B.1}$$

$$\eta=x^*g(t^*)+c,\ s^*=2\lambda\sqrt{t^*}\ \text{and}\ g(t^*)=\frac{1}{\sqrt{2t^*}}\tag{B.2}$$

$$\frac{\partial T_l^*}{\partial t^*} = \frac{\partial T_l^*}{\partial \eta}\frac{\partial \eta}{\partial t^*} = x^*\frac{\partial g}{\partial t^*}\frac{\partial T_l^*}{\partial \eta} \tag{B.3}$$

$$\frac{\partial^2 T_l^*}{\partial x^{*2}} = g^2\frac{\partial^2 T_l^*}{\partial \eta^2} \tag{B.4}$$

$$\frac{\partial T_l^*}{\partial x^*} = g\frac{\partial T_l^*}{\partial \eta} \tag{B.5}$$

$$\frac{\partial s}{\partial t^*} = \frac{\lambda}{\sqrt{t^*}} \tag{B.6}$$

Using the Eqs. (B.1)–(B.6) we will get:

$$\frac{\partial^2 T_l^*}{\partial \eta^2} + 2\frac{\partial T_l^*}{\partial \eta}[\eta - c - \lambda(R-1)] = 0$$

So we are having,

$$\begin{aligned} &c + \lambda(R-1) \to 0 \\ &c = -\lambda(R-1) \end{aligned} \tag{B.7}$$

Using (B.2) and (B.7) we will get:

$$\eta = \frac{x^*}{\sqrt{2t^*}} - \lambda(R-1)$$

References

[1] A. Agarwal, R.M. Sarviya, An experimental investigation of shell and tube latent heat storage for solar dryer using paraffin wax as heat storage material, Eng. Sci. Technol. Int. J. 19 (1) (2016) 619–631.

[2] V. Alexiades, Mathematical Modeling of Melting and Freezing Processes, CRC Press, 1992.

[3] W.D. Bennon, F.P. Incropera, A continuum model for momentum, heat and species transport in binary solid–liquid phase change systems. I. Model formulation, Int. J. Heat Mass Transf. 30 (10) (1987) 2161–2170.

[4] W.D. Bennon, F.P. Incropera, Numerical analysis of binary solid–liquid phase change using a continuum model, Numer. Heat Transf. A Appl. 13 (3) (1988) 277–296.

[5] A. Bermudez, C. Saguez, Numerical simulation of an alloy solidification problem, System Modeling and Optimization, Springer, Berlin Heidelberg, 1982, pp. 318–325.

[6] A. Bhattacharya, P. Dutta, An enthalpy-based model of dendritic growth in a convecting binary alloy melts, Int. J. Numer. Meth. Heat Fluid Flow 23 (7) (2013) 1121–1135.

[7] S. Chakraborty, P. Dutta, An analytical solution for conduction-dominated unidirectional solidification of binary mixtures, Appl. Math. Model. 26 (4) (2002) 545–561.

[8] S. Chakraborty, P. Dutta, The effect of solutal undercooling on double-diffusive convection and macro-segregation during binary alloy solidification: a numerical investigation, Int. J. Numer. Meth. Fluids 38 (9) (2002) 895–917.

[9] S. Chakraborty, P. Dutta, Effects of solutal undercooling on three-dimensional double-diffusive convection and macrosegregation during solidification of a binary alloy, Numer. Heat Transf. A Appl. 48 (3) (2005) 261–281.

[10] M.S. Christenson, F.P. Incropera, Solidification of an aqueous ammonium chloride solution in a rectangular cavity. I. Experimental study, Int. J. Heat Mass Transf. 32 (1) (1989) 47–68.

[11] M.S. Christenson, W.D. Bennon, F.P. Incropera, Solidification of an aqueous ammonium chloride solution in a rectangular cavity. II. Comparison of predicted and measured results, Int. J. Heat Mass Transf. 32 (1) (1989) 69–79.

[12] A.B. Crowley, J.R. Ockendon, Modelling mushy regions, Appl. Sci. Res. 44 (1–2) (1987) 1–7.

[13] E. Jafar-Salehi, M. Eslamian, M.Z. Saghir, Effect of thermo-diffusion on the fluid flow, heat transfer, and solidification of molten metal alloys, Eng. Sci. Technol. Int. J. 19 (1) (2016) 511–517.

[14] P. Levi, N. Ascherson, The Periodic Table, Schocken Books, New York, 1984, p. 34.

[15] M.N. Özişik, Heat Conduction, John Wiley Sons, 1993.

[16] M.N. Özişik, R.L. Murray, On the solution of linear diffusion problems with variable boundary condition parameters, J. Heat Transf. 96 (1) (1974) 48–51.

[17] L. Rubinstein, 'The Stefan Problem' Translations of Mathematical Monographs, vol. 27, American Mathematical Society, Providence, 1971.

[18] J. Stefan, Über die Theorie der Eisbildung, insbesondereüber die Eisbildungim Polarmeere, Ann. Phys. 278 (2) (1891) 269–286.

[19] R.H. Tien, G.E. Geiger, The unidimensional solidification of a binary eutectic system with a time-dependent surface temperature, J. Heat Transf. 90 (1) (1968) 27–31.

[20] V.R. Voller, A similarity solution for solidification of an under-cooled binary alloy, Int. J. Heat Mass Transf. 49 (11) (2006) 1981–1985.

[21] V.R. Voller, An enthalpy method for modeling dendritic growth in a binary alloy, Int. J. Heat Mass Transf. 51 (3) (2008) 823–834.

[22] Y. Yener, M.N. Özişik, On the solution of unsteady heat conduction in multi-region finite media with time dependent heat transfer coefficient, Proceeding of 5th International Heat Transfer Conference, Tokyo, September 3–7, 1974.